

# ISTITUTO NAZIONALE DI FISICA NUCLEARE

Sezione di Catania

---

INFN/BE-94/06  
16 Dicembre 1994

A. Badalà, R. Barbera, A. Palmeri, G.S. Pappalardo, F. Riggi, A.C. Russo,  
G. Russo, R. Turrisi:

**COHERENT PIONS IN NUCLEUS-NUCLEUS COLLISIONS AT  
INTERMEDIATE ENERGIES**

**COHERENT PIONS IN NUCLEUS-NUCLEUS COLLISIONS AT INTERMEDIATE ENERGIES\***

A. Badalà<sup>1</sup>, R. Barbera<sup>1,2</sup>, A. Palmeri<sup>1</sup>, G.S. Pappalardo<sup>1</sup>, F. Riggi<sup>1,2</sup>, A.C. Russo<sup>1</sup>,  
G. Russo<sup>2,3</sup>, R. Turrisi<sup>1,2</sup>

<sup>1</sup> INFN-Sezione di Catania, Corso Italia 57, I-95129 Catania, Italy

<sup>2</sup> Dipartimento di Fisica dell'Università di Catania, Corso Italia 57, I-95129 Catania, Italy

<sup>3</sup> INFN-Laboratorio Nazionale del Sud, Via S. Sofia 44, I-95123 Catania, Italy

**Abstract**

The existing phenomenology concerning subthreshold coherent pion production in nucleus-nucleus collisions at intermediate energy is briefly reviewed together with the presentation of the results of a semi-exclusive experiment which could shed light in disentangling this very peculiar mechanism.

---

\* Expanded version of the talk given by A. Palmeri at the XVII Workshop on Nuclear Physics, Cordoba (Argentina), 1994.

## I. INTRODUCTION

Heavy-ion collisions at energies well above the Coulomb barrier represent a unique tool to study highly excited nuclear matter far from ground-state conditions, i.e. outside the usual domain of existing nuclear structure information. A necessary requirement for the creation of this very interesting microscopic laboratory is the transformation of a large part of the energy from the relative motion during the collision into relatively few final nuclear degrees of freedom. It is in this framework that nonnucleonic probes, like mesons and/or high-energy photons, begin to play a relevant role in the investigation of the properties of the intranuclear collision zone. Pion production in nucleon-nucleus and nucleus-nucleus reactions in the intermediate energy range ( $E_{inc}^{lab}=20-200$  MeV/nucleon), as an example, is of particular interest because it is beyond the kinematic domain accessible in free nucleon-nucleon collisions ( $E_{th}^{lab} \sim 290$  MeV) and, therefore, must involve either the nucleon Fermi motion in both projectile and target and/or more collective/coherent effects implying the combined action of more than two colliding nucleons.

In this contribution we present a brief report on the current status of the search for coherent pion production in nucleus-nucleus collisions at intermediate energies. The paper is organized as follows. Section II contains a critical outline of the already existing phenomenology (together with its theoretical interpretation) concerning both light and heavy-ion induced reactions investigated through inclusive as well as exclusive experiments. In Sec. III the results of a recent new-generation semi-exclusive experiment showing the evidence of coherent pion production are presented. Conclusions are given in Sec. IV.

## II. THE STATUS-OF-THE-ART

### A. Light-ion reactions

#### 1. Exclusive experiments

Since its theoretical suggestion, given in 1947 by McMillan and Teller [1], subthreshold coherent pion production has been firstly evidenced in light-ion collisions induced by protons [2-4] and light nuclei (up to  $^4\text{He}$ ) [5-8] on light targets (up to  $^{12}\text{C}$ ). The bombarding energies were included between 90 and 200 MeV/nucleon, in all cases very close to the absolute production threshold.

This particular kinematical constraint was been intentionally imposed in order to study the so-called “pionic fusion” (sometimes referred to as doubly coherent pion production), a fully coherent process where both projectile ( $A_1$ ) and target ( $A_2$ ) fuse into a specific bound state of the final nucleus ( $A_1 + A_2 \rightarrow B(E^*) + \pi$ ) converting all the kinetic energy of the

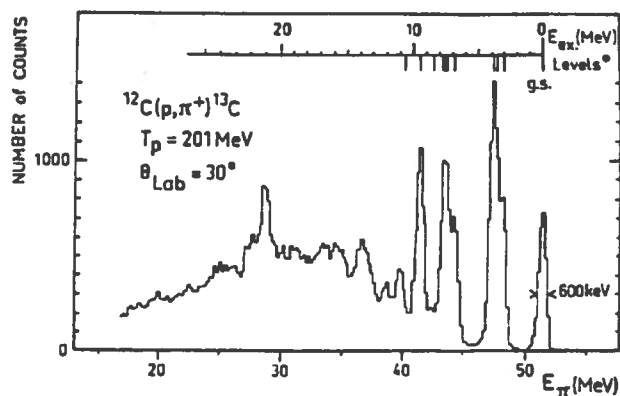


FIG. 1. Spectrum of pions produced at  $30^\circ$  in the  $^{12}\text{C}(p, \pi^+)^{13}\text{C}$  reaction at  $E_p=201 \text{ MeV}$  [4]. The lowest energy levels of  $^{13}\text{C}$  are marked in the upper excitation energy scale.

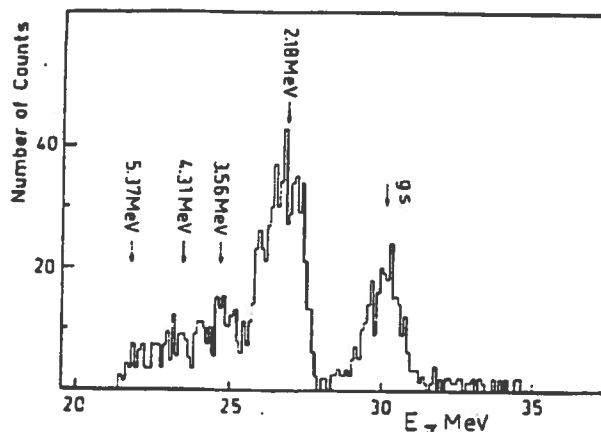


FIG. 2. Spectrum of pions produced at  $20^\circ$  in the  ${}^3\text{He}({}^3\text{He}, \pi^+){}^6\text{Li}$  reaction at  $E_{He} = 94$  MeV/nucleon [6]. The vertical arrows mark the positions of the lowest energy levels of  ${}^6\text{Li}$ .

entrance channel in the creation of one pion. As an example, Figs. 1 and 2 show the pion energy spectra (measured at different detection angles) relative to the reactions  ${}^{12}\text{C}(p, \pi^+){}^{13}\text{C}$  at  $E_p = 201$  MeV [4] and  ${}^3\text{He}({}^3\text{He}, \pi^+){}^6\text{Li}$  at  $E_{He} = 94$  MeV/nucleon [6]. Both plots clearly exhibit a discrete structure with the peak of the ground state and those relative to the first excited states of the residual nucleus. This energy transfer between two well-defined degrees of freedom excludes a fully developed thermalization process and, consequently, a statistical approach is inadequate for such an exclusive process since all the nucleons must contribute cooperatively. Pionic fusion has been tentatively explained in the past within a theoretical model [9] which, starting from a microscopic nucleon–nucleon interaction, leads to an effective coupling of the pion field to the relative motion of the two fragments. An initial  $\Delta$ -excitation propagates in the final nucleus and decays by emitting the pion. Figure 3 shows the comparison between the experimental angular distributions of some excited states of the  ${}^6\text{Li}$  created in the reaction  ${}^3\text{He}({}^3\text{He}, \pi^+){}^6\text{Li}$  at  $E_{He} = 94$  MeV/nucleon [6] and those calculated by the model described in Ref. [9]. The agreement is fair in view of the complexity of the reaction.

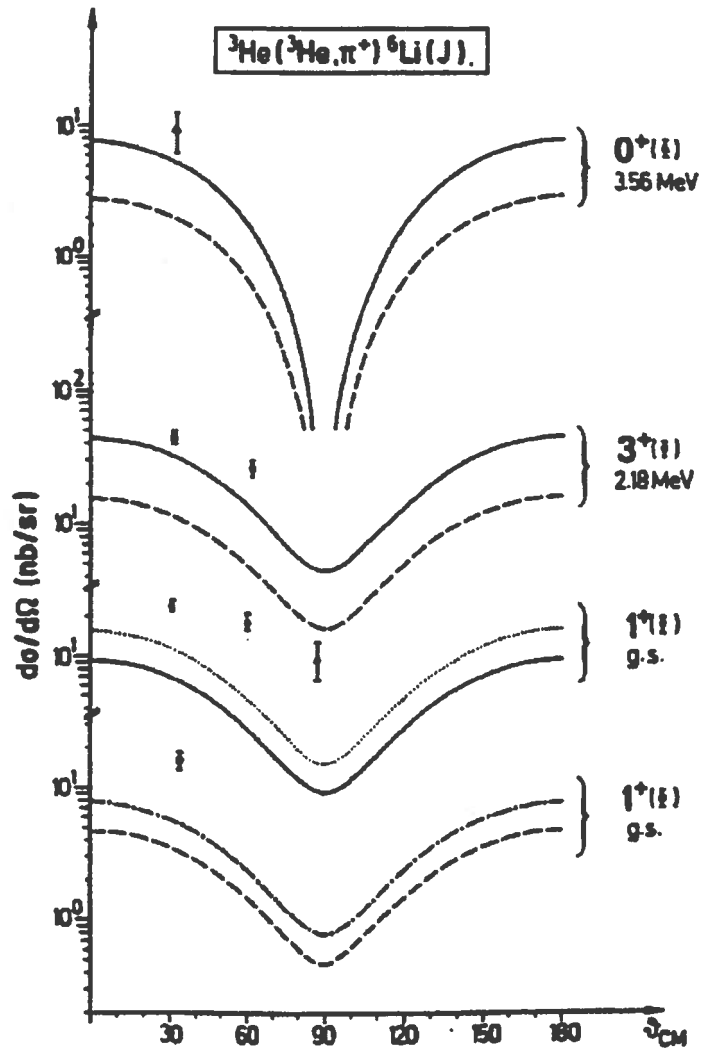


FIG. 3. Differential cross section for various final states evaluated with the model of Ref. [9]. Solid (dashed) curve for  $E_{He}=282$  (265) MeV; dotted (dash-dotted) curve is the result for a 10%  $D$ -state in the ground state for 282 (262.5) MeV. Experimental data come from Ref. [6].

The cooperative character of doubly coherent pion production mechanisms, responsible of the large demanded momentum transfer, also emerges from the analysis of the cross sections. Experimental results show that they are sharply decreasing with the increase of the target mass: more than three orders of magnitude passing from  ${}^3\text{He}({}^3\text{He},\pi^+){}^6\text{Li}$  [6] and  ${}^4\text{He}({}^3\text{He},\pi^+){}^7\text{Li}$  [7] reactions to  ${}^6\text{Li}({}^3\text{He},\pi^+){}^9\text{Be}$  [8] and  ${}^{10}\text{B}({}^3\text{He},\pi^+){}^{13}\text{C}$  [8] ones at the same incident energy. A smooth decrease of the cross section is also evidenced with the increase of the bombarding energy [8], thus demonstrating the strong link between the probability of the process and the smallness of the final available phase space.

## 2. Inclusive experiments

Experimental evidences of cooperative effects in light-ion-induced subthreshold pion production are not only restricted to fusion reactions. Mean field components have been, in fact, also observed in inclusive proton-induced reactions on two isotopes of Nickel [10,11]. Figures 4 and 5 show the comparison of typical charged-pion energy spectra from the  ${}^{58}\text{Ni}(p,\pi^\pm)\text{X}$  and  ${}^{64}\text{Ni}(p,\pi^\pm)\text{X}$  reactions at  $E_p=201$  MeV. The energy scales are shifted by the differences in  $Q_{gg}$  in order to compare both shapes and yields of the spectra at the same excitation energy of the residual system ( $Q_{gg}$  is the Q-value of the two-body reaction in which the pion is emitted). The high-energy parts coincide for both isotopes, for a given pion charge, but the  $\pi^+$  yield is almost a factor of 10 larger than the  $\pi^-$  one. The differences which appear in the low-energy parts are due to the different values of  $Q_{gg}$  which constrain the fall-off to zero of the cross sections at different excitation energies for the various residual nuclei. As a consequence, the integrated total cross sections cover different energy ranges due to the different kinematical limits and the total cross sections, obtained from a double integration over energy and angle (using a low-energy extrapolation following the dashed lines drawn in Figs. 4 and 5) [10], are observed to vary in the same sense as  $Q_{gg}$ .

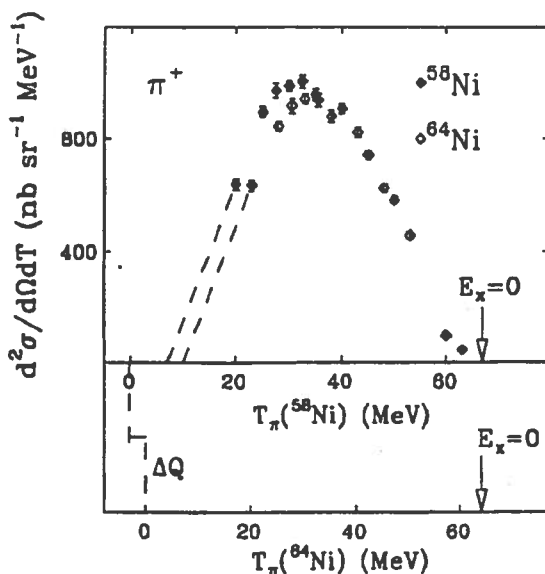


FIG. 4. Energy spectra at  $22^\circ$  of positive pions from the  $^{58}\text{Ni}(p,\pi^+)X$  (filled diamonds, higher energy scale) and  $^{64}\text{Ni}(p,\pi^+)X$  (empty diamonds, lower energy scale) reactions at  $E_p=201$  MeV [10,11]. The energy spectrum relative to the  $^{64}\text{Ni}$  target is shifted by  $\Delta Q$  (see text).

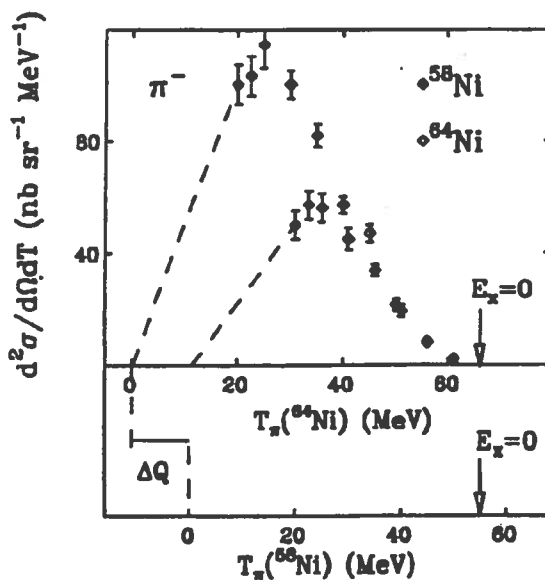


FIG. 5. Energy spectra at  $22^\circ$  of negative pions from the  $^{58}\text{Ni}(p,\pi^-)X$  (filled diamonds, lower energy scale) and  $^{64}\text{Ni}(p,\pi^-)X$  (empty diamonds, higher energy scale) reactions at  $E_p=201$  MeV [10,11]. Unlike Fig. 4, in this case the energy spectrum relative to the  $^{58}\text{Ni}$  target is shifted by  $\Delta Q$  (see text).



## B. Heavy-ion reactions

### 1. Inclusive experiments

The availability, in the late seventies, of heavy-ion beams at intermediate energies allowed for the first observation of inclusive subthreshold pion production in heavy-ion collisions [12]. Since then, this subject has been investigated with a large variety of projectile/target combinations in the bombarding-energy range between 20 and around 200 MeV/nucleon [13–21]. Side by side, many theoretical approaches have been undertaken [22–37], sometimes even starting from opposite hypotheses, ranging from nucleon–nucleon–collision models [22–25], intranuclear cascade models [26,27], and cooperative phase–space models [28] to participant–spectator thermodynamic models [29–34] and coherent (*bremstrahlung*) models [35–37].

Figure 6 shows the neutral pion production excitation function below 100 MeV/nucleon. Cross sections have been scaled by the quantity  $(A_p A_t)^{2/3}$ , in order to compare data relative to different  $A_p + A_t$  systems. It is worth observing that, in accordance with the *subthreshold* character of pion production at these bombarding energies, the value of the total cross section decreases by about five orders of magnitude in a range of just 60 MeV/nucleon. Different curves refer to the theoretical calculation of some of the aforementioned models. Higher energy data (i.e., above 60 MeV/nucleon) are quite insensible to the different theoretical assumptions, except the first–collision model (dotted line) which is very far from the points and, even, does not foresee at all pion production below 50 MeV/nucleon. At lower energies, on the contrary, all calculations underestimate the experimental values of the total cross section. The disagreement is not limited to integral observables such as  $\sigma_{\pi}^{tot}$  but, nay, it is more evident in energy spectra and angular distribution comparison [15,20,21].

This behaviour can be qualitatively explained by means of simple energetic considerations. When the bombarding energy is near 100 MeV/nucleon, the total available energy in the center of mass is much larger than the total energy of the created pion and the phase–space volume after its emission is still very large. In these conditions many channels are simultaneously open and the poor definition of the final state, typical of inclusive

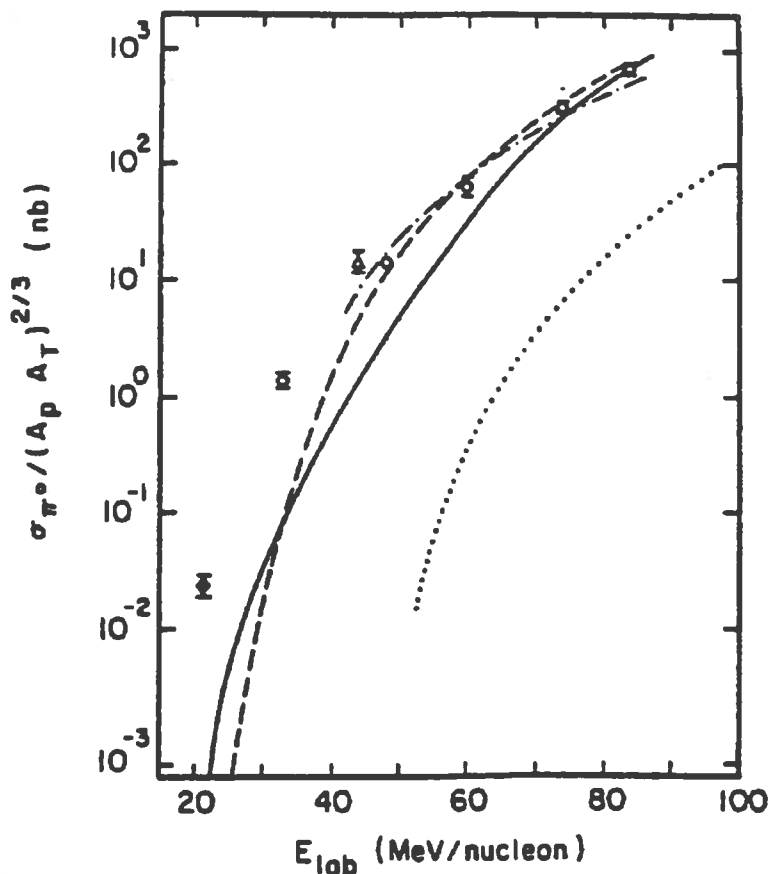


FIG. 6. Pion-production total cross-section, divided by  $(A_p A_T)^{2/3}$ , as a function of the bombarding energy per nucleon [21]. Experimental data come from Refs. [16] (open triangle), [18] (open circles), and [21] (closed diamond). Also shown are the results of a single nucleon-nucleon hard scattering model [24] (dotted line), the extended phase-space model [28] (dashed line), a thermal model [31] (solid line), and the *bremsstrahlung* model [35-37] (dashed dotted line).

experiments, does not allow for disentangle among the various theoretical model. On the contrary, as far as the bombarding energy decreases, the phase-space volume shrinks and true cooperative effects begin to be relevant. In order to facilitate the comprehension of this point, Fig. 7 shows center-of-mass pion energy spectra as a function of the energy available in the center of mass after pion emission [21]. This quantity equals the total center-of-mass energy, corrected for the  $Q$ -value, minus the pion total energy. The zero on the scale indicates the kinematical limit, where the pion carries away all the available energy. To keep homogeneous the comparison with Fig. 6, all data plotted in Fig. 7 belong to the same range

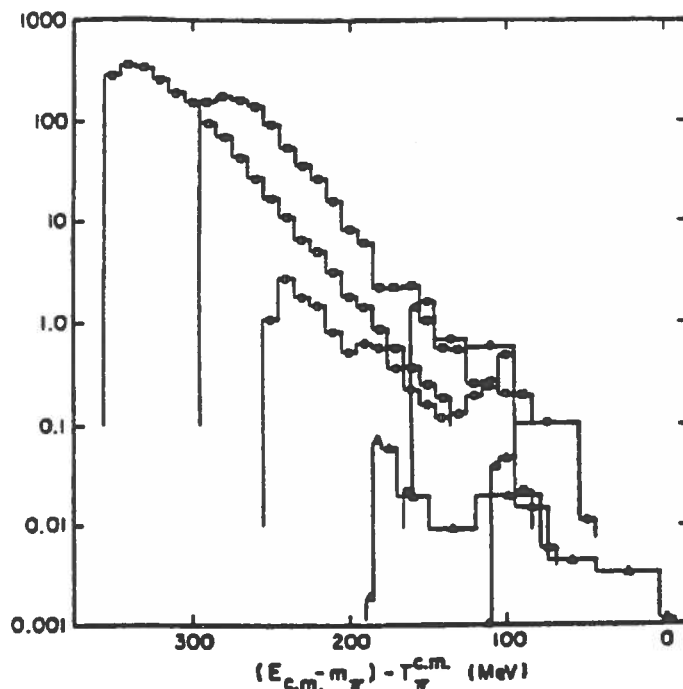


FIG. 7. Pion kinetic energy spectra as a function of the energy available in the center-of-mass system after pion emission [21]. Experimental data come from Refs. [21] (closed and open triangles), and [18] (all other symbols).

of bombarding energy. Near the phase-space limit, all data, referring to different systems at different energies, tend to merge together. Here, the pion differential cross sections scale with the full center-of-mass energy, while at higher energies they scale with the energy per nucleon or, at most, the kinetic energy of a few nucleons. Thus, near the absolute threshold, the scaling with the total energy coupled with the failure of single nucleon-nucleon collision and cooperative or statistical models emphasizes the need for a fully coherent mechanism to describe pion production.

The same conclusion can be reached looking at Fig. 8 where the pion energy spectrum relative to the reaction  $\text{Al}(^{16}\text{O}, \pi^0)\text{X}$  at 25 MeV/nucleon [20] is reported. The upper scale is the fraction of the center-of-mass energy required to produce a neutral pion travelling at  $0^\circ$  in the laboratory. It is easy to observe that values of this quantity up to 75% can be obtained.

Then, in conclusion, inclusive experiments clearly exhibit the possibility of coherent pion production but exclusive experiments are claimed to disentangle the involved mechanism.

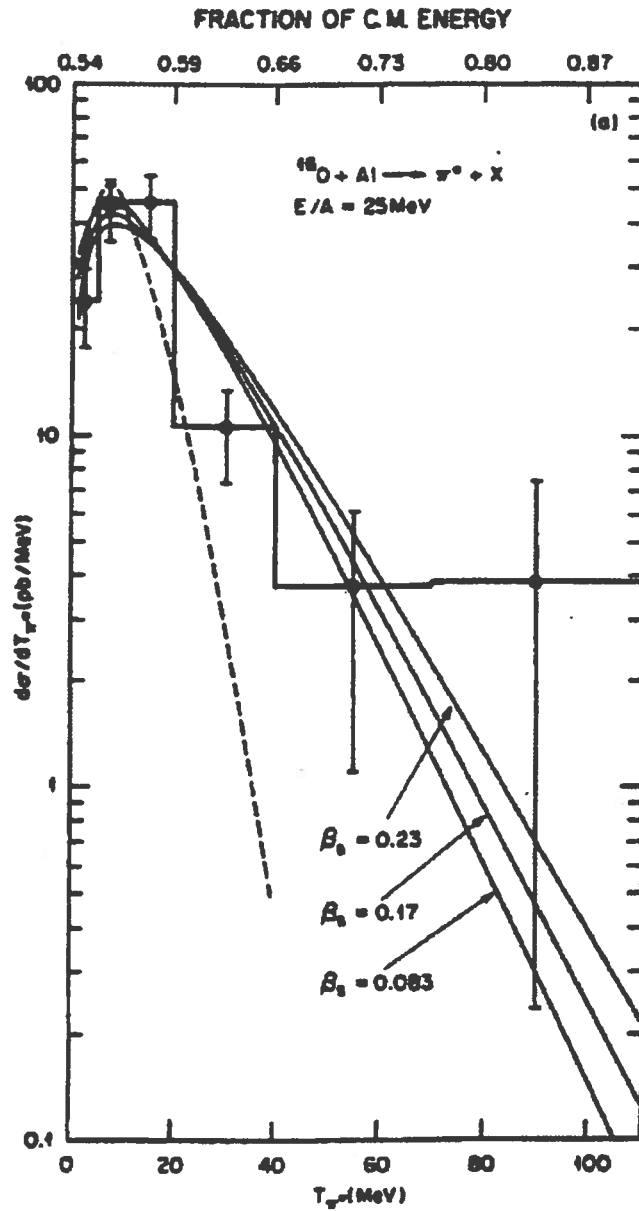


FIG. 8. Laboratory energy distribution of neutral pion coming from the reaction  $^{27}\text{Al}(^{16}\text{O}, \pi^0)\text{X}$  at  $E_0 = 25$  MeV/nucleon [20]. The dashed line is the prediction of the model of Ref. [28] multiplied by a factor of 50. Solid lines are the predictions of a simple thermal model based on the results of a moving source analysis [20]. The legend at the top of the figure is the fraction of the center-of-mass energy required to produce a  $\pi^0$  traveling at  $0^\circ$  in the laboratory.

## 2. Exclusive experiments

As it has been observed in the previous subsection, the main drawback of inclusive experiments concerning pion production is the lack of characterization of the final state of the collision (both in configuration and momentum space) that provides useful information about the reaction mechanism and, hence, a clear experimental proof capable to distinguish, in this kind of measurements, coherent pion production from other channels is very difficult to obtain. For this reason, many exclusive experiments have been performed, in these last ten years, to detect pions in coincidence with charged particles [38–44] and fission fragments [45]. The used bombarding energies have been, in all cases, greater than or equal to about 100 MeV/nucleon. The most important result, common to all these experiments, is that pions are preferentially produced in central collisions where it is possible to realize a large overlap of the projectile and target density distributions.

The main part of the existing experimental phenomenology has been successfully reproduced, both qualitatively and quantitatively [43,44,46,47], within microscopic transport models [46] based on *in medium* incoherent nucleon–nucleon collisions and taking into account final state effects as Pauli–blocking and pion reabsorption (see especially Ref. [43,44]). As a reference example, Fig. 9 shows the comparison between the experimental energy–angle double differential cross sections of pions emitted in the  $^{27}\text{Al}(^{36}\text{Ar},\pi^0)\text{X}$  reaction at 95 MeV/nucleon [44] (points) and those resulting from a theoretical calculation based on the solution of the Boltzmann–Nordheim–Vlasov (BNV) equation [44,48] (solid and dashed histograms). Dashed histograms are the pure results of the calculation, while solid ones include the effect of pion reabsorption in nuclear medium, treated on an event–by–event basis.

The agreement between experimental data and theoretical calculations reduces to a very small amount the contribution of any coherent channel for pion production, unlike what was inferred from the analysis of inclusive data belonging to the same energetic domain (see Fig. 6). This is due to the high value of the bombarding energy and to the geometrical characteristics of the reaction. In central collisions at intermediate energies, in fact, both

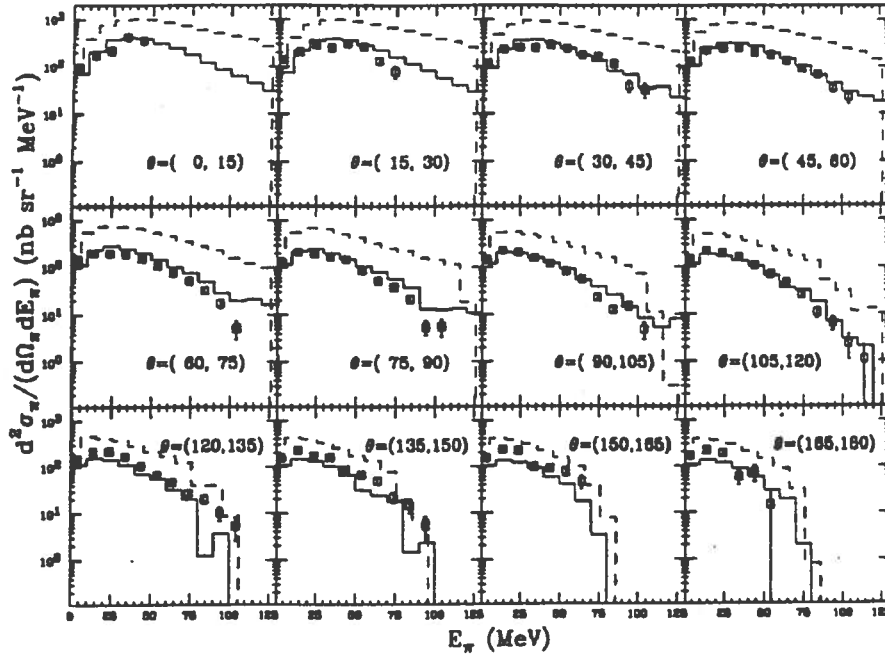


FIG. 9. Comparison between experimental (points) pion energy spectra at different detection angles relative to the  $^{27}\text{Al}(^{36}\text{Ar}, \pi^0)\text{X}$  reaction at  $E_{\text{Ar}}=94$  MeV/nucleon [44] and the results of a BNV dynamical calculation [44,48] taking also into account the effect of pion reabsorption in the nuclear medium (solid histograms). The dashed histograms represent the BNV calculation without reabsorption effect.

projectile and target generally break up into many pieces and lose their identity. Thus, the observation of only a part of them in coincidence with a pion, as in all experiments realized so far, cannot prove unambiguously the original mechanism, since it is not possible to attribute an incompletely described final state of the reaction to a well defined process. In order to look for possible coherent phenomena in subthreshold pion production, it is, then, evident the need of a detailed knowledge of the many-body distribution function  $f(\vec{r}_n, \vec{p}_n, t)$  in the phase-space for  $t \rightarrow +\infty$ .

The first attempt in this direction has been made by Erazmus *et al.* [49], who tried to measure the neutral pion production in the reaction  $^{12}\text{C}+^{12}\text{C} \rightarrow ^{12}\text{C}(J^\pi=1^+, T=1, E^*=15.1 \text{ MeV}) + \pi^0 + \text{X}$  at 95 MeV/nucleon, where a Gamow-Teller transition ( $\Delta S=\Delta T=1$ ) excites the projectile to the  $J^\pi=1^+, T=1$  state which preferentially decays by the emission

of a  $M1$  photon of 15.1 MeV. The importance of this particular channel, which suggested its choice, is due to the fact that pion production in such peripheral heavy-ion collisions can be explained by means of coherent excitations of spin-isospin modes through the  $\Delta$ -hole channel in either projectile and target [50–52]. It is worth noting that this reaction satisfies the aforementioned necessary condition of completeness of the final state since a full identification of the process is achieved by the quadruple-coincidence measurement of the outgoing ejectile ( $^{12}\text{C}$ ), the 15.1-MeV photon, and the two high-energy photons coming from the  $\pi^0$  decay. Unfortunately, in the reported experiment [49], only one high-energy photon ( $E_\gamma > 30$  MeV) was detected together with the residual nucleus and the decay  $\gamma$ -ray and the found 9 good events (over a background of less than 0.01 events) allowed only for the evaluation of an upper limit for the total cross section. Notwithstanding this limitation, the found value of 60 nb, which is about  $10^{-3}$  times the total pion cross section, is in reasonable agreement with the theoretical calculations performed in Ref. [52] for the same system at the same bombarding energy.

Isobar production related to isovector collective state decay is not, however, the only possible way to coherently produce a pion. In the next section we will show the results of a completely different experiment, realized with a similar projectile ( $^{16}\text{O}$ ) at the same bombarding energy, aimed to evidence a coherent behaviour of the projectile in the nuclear field of the target [53].

### III. A NEW EXPERIMENT

In these last years, a large amount of both experimental [54] and theoretical [55] work has been devoted to the study of projectile breakup in light- and medium-heavy-ion collisions at intermediate energies. This has permitted to investigate on very important subjects such as the space-time evolution of the interacting system and the existence of a limit for the excitation energy that a nucleus can sustain before its breaking. Projectile disassembly channels, involving only charged particles, have been observed in those events where the total detected charge was equal to the projectile one (relatively complete events). Some

physical quantities concerning the whole primary projectile-like nucleus, like its velocity and excitation energy distributions, have been reconstructed from the measured kinetic energies of all detected fragments in their center-of-mass frame.

In this section we show the results of an experiment in which the 4-He breakup of the  $^{16}\text{O}$  projectile has been observed in coincidence with the emission of a charged pion in reactions induced on an  $^{27}\text{Al}$  target at 94 MeV/nucleon [53]. Obviously, the observation of a pion in these breakup reactions gives a clue of the existence of coherent production mechanisms.

#### A. The experimental set-up

The overall detection apparatus is drawn in Fig. 10. It consists of a *range* telescope of 10 plastic scintillators, used to detect charged pions of kinetic energy ranging from 23.4 MeV up to 74.1 MeV at laboratory angles  $\theta=70^\circ$ ,  $\theta=90^\circ$  and  $\theta=120^\circ$ , and a forward wall of 96 plastic scintillators, called *Mur*, to detect light charged particles in the whole fraction of the total solid angle between  $\theta=3^\circ$  and  $\theta=30^\circ$ . Detailed descriptions of the two detectors can be found in Refs. [42,56,57].

All particles different from pions impinging on the telescope have been on-line rejected by a suitable adjusting of the discriminator thresholds. The residual contaminants (mainly electrons and not rejected protons) have been eliminated in the off-line data reduction performing a multiple  $\Delta E-E$  and  $\Delta E-\Delta E$  analysis of the relative energy loss in each scintillator element of the telescope.

Light fragments, whose charge is included between  $Z=1$  and  $Z=8$ , have been identified in the *Mur* by means of a standard  $\Delta E$ -TOF technique. A very clean separation of the different charges has been possible only for particles crossing the scintillators, while those stopped in the detectors could not be easily identified [58]. Only charge identified particles have been taken into account and, hence, a velocity threshold of about 5 cm/ns, due to the thickness of the detectors, has been imposed on the data.

The analysis has been restricted only to those  $\pi^\pm \cap 4\text{He}$  coincidence events where all four  $Z=2$  particles impinging on the *Mur* have  $v_{He} > 8$  cm/ns and  $\theta_{He} \leq 16.5^\circ$ . These severe



## EXPERIMENTAL SETUP

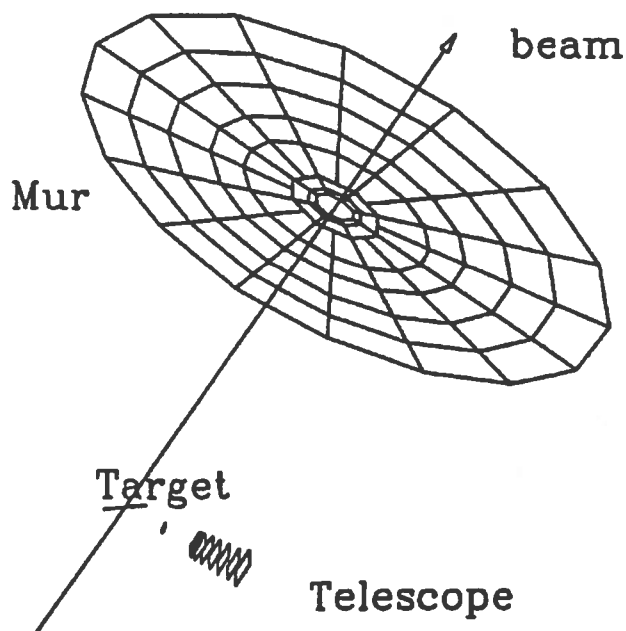


FIG. 10. Global view of the experimental set-up.

conditions have been chosen to select those events resulting from the breakup of the primary projectile-like nucleus [54], in which there is the minimum contamination due to fragments coming from more relaxed sources relative to different mechanisms at smaller impact parameters [59]. It is in this framework that we speak about peripheral pion production in projectile breakup reactions. In order to increase the statistics as much as possible, both pion charge states and detection angles are summed up. The contribution of random coincidences has been statistically evaluated by counting the number of  $\pi^{\pm}\cap^4\text{He}$  events contained in the spurious coincidence peaks of the time-of-flight spectrum of each detector of the *Mur* [58] but none of these events has been found.

## B. Results

Using standard relativistic kinematics, we have reconstructed, on an event-by-event basis, the projectile-like nucleus velocity ( $v_{PLN}$ ) defined as that of the center of mass of the four He ions detected in each event. Figure 11 shows the distribution of this quantity for inclusive (upper part) [54] and coincidence events (lower part). Right and left arrows indicate projectile and compound nucleus velocities, respectively. The inclusive velocity distribution has the usual shape observed in projectile fragmentation at the intermediate energies. The centroid of the PLN velocity spectrum is slightly lower than the beam velocity in agreement with the existing phenomenology. The net effect of a charged pion detected in coincidence with the four He ions is to shift the velocity spectrum to lower values. The peaks of the PLN velocity spectra of Fig. 11 are shifted by about 1.5 cm/ns which is, at these velocities, more than five times the velocity experimental uncertainties. This corresponds to a projectile energy loss of 200–250 MeV, large enough to produce a charged pion in the measured kinetic energy range. So, by detecting all projectile breakup fragments inclusively and in coincidence with the pion and measuring their velocities, we are able to select, for the first time, a well defined class of events in which the total pion energy (which is an appreciable fraction of the energy available) is provided by the coherent slowing down of the projectile.

Notwithstanding the coherent process discussed above is energetically possible, the found number of true coincidences (18 events) is very small as compared to the total number of detected pions ( $\sim 1.4 \cdot 10^4$ ) and, therefore, we have performed several tests [53] in order to verify that the particles observed in the  $\pi^\pm \cap 4\text{He}$  events were really pions and to check whether light charged particles hitting the *Mur* in coincidence with a pion effectively come from the slowed down projectile or from a more relaxed source (*fireball*) [59] (i.e., from more central collisions). None of these tests has invalidate the experimental evidence. It is worth noting that, also in this case, with a completely different process under study, coherent contribution is  $10^3$  times smaller than the total pion cross-section.

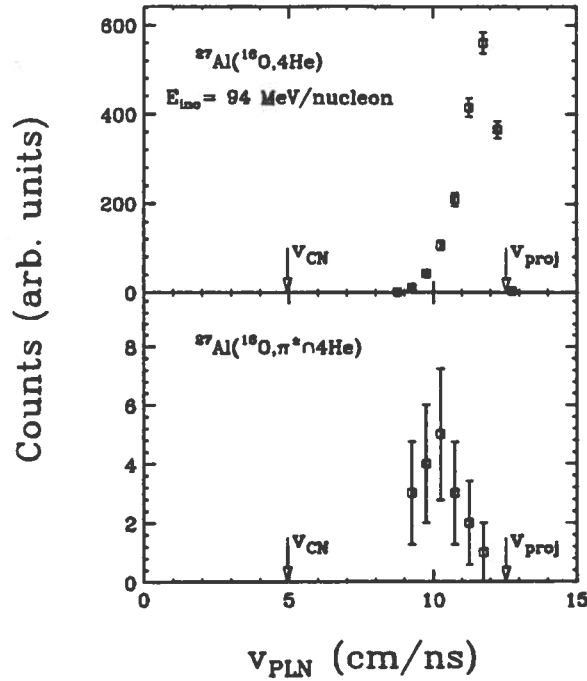


FIG. 11. Projectile-like nucleus velocity distributions for 4-He inclusive breakup events (upper part) and for coincidence ones (lower part). In each plot right and left arrows indicate the projectile velocity and the compound nucleus velocity, respectively. Data come from Ref. [53].

As an ulterior confirmation of the coherent character of the observed pion production, Fig. 12 shows the total (left part) and single fragment (right part) experimental parallel momentum distributions for inclusive 4-He breakup events (upper part) and for  $\pi^\pm n 4\text{He}$  coincidence ones (lower part). All momenta are normalized to the projectile momentum ( $p_b$ ). In both cases coincidence distributions are shifted toward lower parallel momentum values with respect to the inclusive distributions. From the weighted mean values of these distributions, it is easy to calculate [53] that  $[\langle \sum (p_{||}/p_b) \rangle_{4\text{He}} - \langle \sum (p_{||}/p_b) \rangle_{\pi^\pm n 4\text{He}}] \simeq 4 \cdot [\langle p_{||}/p_b \rangle_{4\text{He}} - \langle p_{||}/p_b \rangle_{\pi^\pm n 4\text{He}}]$  thus indicating that the slowing down of the center of mass of the four He ions detected in coincidence events is due to coherent slowing down of each of these particles.

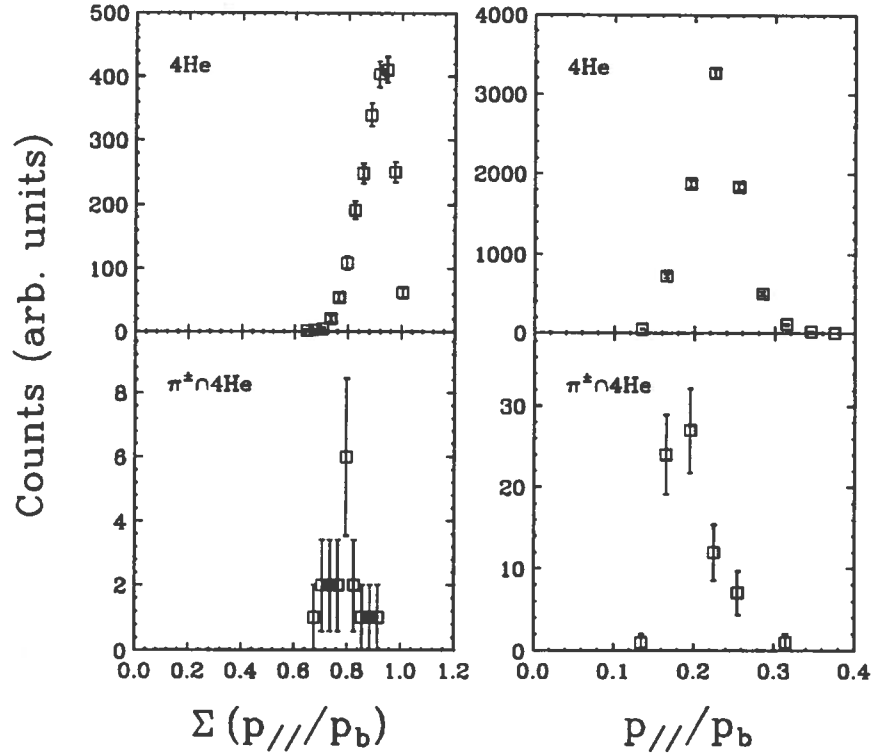


FIG. 12. Total (left part) and single fragment (right part) parallel momentum distributions for  $4\text{He}$  inclusive breakup events (upper part) and for  $\pi^\pm \cap 4\text{He}$  coincidence ones (lower part). All momenta are divided by that of the projectile ( $p_b$ ). Data come from Ref. [53].

#### IV. CONCLUSION AND OUTLOOK

A few pages are largely insufficient to exhaustively describe the huge phenomenology concerning the search for coherent subthreshold pion production in heavy-ion collisions at intermediate energies. Anyway, the most important conclusion of this brief report is that new exclusive experiments could really open concrete possibilities in this field through the strong characterization of the final state of the reaction when a pion is created. Considering (i) that any incoherent microscopic calculation based on the solution of transport equations only holds if the center-of-mass energy of the two colliding ions is significantly higher than the

pion total energy, and, vice versa, (ii) that all coherent models, such as the *bremstrahlung* model and/or the isobaric one, presuppose a sizeable effect of the pion creation on the projectile velocity, next years should see the realization of exclusive experiments in the lowest possible bombarding energy regime. Furthermore, it should have particular interest the careful determination of the shapes of both pion differential energy spectrum and angular distribution (better if with respect to the reaction plane) in order to univocally determine the underlying reaction mechanism.

## REFERENCES

- [1] W. G. McMillan and E. Teller, *Phys. Rev.* **72**, 1 (1947).
- [2] S. Dahlgren, P. Grafström, B. Höistad, and A. Åsberg, *Nucl. Phys. A* **204**, 53 (1973).
- [3] S. Dahlgren, P. Grafström, B. Höistad, and A. Åsberg, *Nucl. Phys. A* **211**, 243 (1973).
- [4] L. Bimbot *et al.*, *Nucl. Phys. A* **440**, 636 (1985).
- [5] N. S. Wall, J. N. Craig, and D. Ezrow, *Nucl. Phys. A* **268**, 459 (1976).
- [6] Y. Le Bornec, L. Bimbot, N. Koori, F. Reide, A. Willis, N. Willis, and C. Wilkin, *Phys. Rev. Lett.* **47**, 1870 (1981).
- [7] L. Bimbot, M. P. Combes, J. C. Jourdain, Y. Le Bornec, F. Reide, A. Willis, N. Willis, J. F. Germond, and C. Wilkin, *Phys. Lett. B* **114**, 311 (1982).
- [8] N. Willis, L. Bimbot, T. Hennino, J. C. Jourdain, Y. Le Bornec, and F. Reide, *Phys. Lett. B* **136**, 334 (1984).
- [9] K. Klingenberg, M. Dillig, and M. G. Huber, *Phys. Rev. Lett.* **47**, 1654 (1981).
- [10] A. Palmeri, S. Aiello, A. Badalà, R. Barbera, G. S. Pappalardo, L. Bimbot, F. Reide, N. Willis, and H. Oeschler, *Phys. Rev. C* **40**, 1081 (1989).

- [11] A. Badalà, R. Barbera, A. Palmeri, G. S. Pappalardo, F. Riggi, A. Adorno, A. Bonasera, and L. Bimbot, *Phys. Rev. C* **46**, 604 (1992).
- [12] W. Benenson *et al.*, *Phys. Rev. Lett.* **43**, 683 (1979).
- [13] T. Johansson *et al.*, *Phys. Rev. Lett.* **48**, 732 (1982).
- [14] S. Nagamiya *et al.*, *Phys. Rev. Lett.* **48**, 1780 (1982).
- [15] V. Bernard *et al.*, *Nucl. Phys. A* **423**, 511 (1984).
- [16] H. Heckwolf *et al.*, *Z. Phys. A* **315**, 243 (1984).
- [17] P. Braun-Munzinger, P. Paul, L. Ricken, J. Stachel, P. H. Zhang, G. R. Young, F. E. Obenshain, and E. Grosse, *Phys. Rev. Lett.* **52**, 255 (1984).
- [18] H. Noll *et al.*, *Phys. Rev. Lett.* **52**, 1284 (1984).
- [19] E. Chiavassa *et al.*, *Nucl. Phys. A* **422**, 621 (1984).
- [20] G. R. Young, F. E. Obenshain, F. Plasil, P. Braun-Munzinger, R. Freifelder, P. Paul, and J. Stachel, *Phys. Rev. C* **33**, 742 (1986).
- [21] J. Stachel *et al.*, *Phys. Rev. C* **33**, 1420 (1986).
- [22] G. F. Bertsch, *Phys. Rev. C* **15**, 713 (1977).
- [23] R. Shyam and J. Knöll, *Phys. Lett. B* **136**, 221 (1984).
- [24] C. Guet and M. Prakash, *Nucl. Phys. A* **428**, 119c (1984).
- [25] H. Cruse, *Phys. Rev. Lett.* **54**, 289 (1985).
- [26] M. Blann, *Phys. Rev. Lett.* **54**, 2215 (1985).
- [27] M. Blann, *Phys. Rev. C* **32**, 1231 (1985).
- [28] R. Shyam and J. Knöll, *Nucl. Phys. A* **426**, 606 (1984).
- [29] J. Aichelin and G. F. Bertsch, *Phys. Lett. B* **138**, 350 (1984).

- [30] J. Aichelin, *Phys. Rev. Lett.* **52**, 2340 (1984).
- [31] M. Prakash *et al.*, *Phys. Rev. C* **33**, 937 (1986).
- [32] A. Bonasera *et al.*, *Nucl. Phys. A* **463**, 653 (1987).
- [33] A. Bonasera *et al.*, *Nucl. Phys. A* **483**, 738 (1988).
- [34] A. Adorno *et al.*, *Nucl. Phys. A* **488**, 451c (1988).
- [35] D. Vasak *et al.*, *Phys. Scr.* **22**, 25 (1980).
- [36] D. Vasak *et al.*, *Nucl. Phys. A* **428**, 291c (1984).
- [37] T. Stahl *et al.*, *Z. Phys. A* **327**, 311 (1987).
- [38] J. Miller *et al.*, *Phys. Rev. Lett.* **58**, 2408 (1987).
- [39] S. Aiello *et al.*, *Europhys. Lett.* **6**, 25 (1988).
- [40] G. Sanouillet *et al.*, *Il Nuovo Cimento A* **99**, 875 (1988).
- [41] A. Badalà, R. Barbera, G. Bizard, J. L. Laville, A. Palmeri, and G. S. Pappalardo, *Nucl. Phys. A* **482**, 511 (1988).
- [42] A. Badalà *et al.*, *Phys. Rev. C* **43**, 190 (1991).
- [43] A. Badalà *et al.*, *Phys. Rev. C* **47**, 231 (1993).
- [44] A. Badalà *et al.*, *Phys. Rev. C* **48**, 2350 (1993).
- [45] B. Erasmus *et al.*, *Nucl. Phys. A* **481**, 821 (1988).
- [46] W. Cassing, V. Metag, U. Mosel, and K. Niita, *Phys. Rep.* **188**, 363 (1990), and reference therein.
- [47] V. Metag, *Prog. Part. Nucl. Phys.* **30**, 75 (1993).
- [48] A. Bonasera, G. Russo, and H. H. Wolter, *Phys. Lett. B* **246**, 337 (1990).

- [49] B. Erasmus *et al.*, Phys. Rev. C **44**, 1212 (1991).
- [50] P. A. Deutchman and L. W. Townsend, Phys. Rev. C **25**, 1105 (1982).
- [51] P. A. Deutchman, J. W. Norbury, and L. W. Townsend, Nucl. Phys. A **454**, 733 (1986).
- [52] C. Guet, M. Soyeur, J. Bowlin, and G. E. Brown, Nucl. Phys. A **494**, 558 (1989).
- [53] A. Badalà, R. Barbera, A. Palmeri, G. S. Pappalardo, F. Riggi, A. C. Russo, G. Russo, R. Turrisi, G. Bizard, and J. L. Laville, Phys. Lett. B **316**, 240 (1993).
- [54] For a review see, e.g.: A. Badalà, R. Barbera, A. Palmeri, G. S. Pappalardo, F. Riggi, G. Polarolo, and C. H. Dasso, Phys. Lett. B **299**, 11 (1993); A. Badalà, R. Barbera, A. Palmeri, G. S. Pappalardo, and F. Riggi, Phys. Rev. C **48**, 633 (1993), and references therein.
- [55] H. Fuchs and K. Möhring, Rep. Prog. Phys. **57**, 231 (1994).
- [56] J. Julien, in *Proceedings of the 3rd Intern. Conf. on Nuclear reaction mechanism*, (Varenna, Italy, 1982).
- [57] G. Bizard, A. Drouet, F. Lefebvres, J. P. Patry, B. Tamain, F. Guilbault, and C. Lebrun, Nucl. Instrum. Methods A **244**, 483 (1986).
- [58] D. Durand *et al.*, Nucl. Phys. A **511**, 442 (1990).
- [59] R. Barbera *et al.*, Nucl. Phys. A **518**, 767 (1990).